

## Composite particles and entropy production in relativistic nuclear collisions

K. G. R. Doss,<sup>(a)</sup> H.-Å. Gustafsson,<sup>(b)</sup> H. H. Gutbrod,<sup>(b)</sup> B. Kolb,<sup>(b)</sup>  
 H. Löhner,<sup>(b)\*</sup> B. Ludewigt,<sup>(b)†</sup> A. M. Poskanzer,<sup>(a)</sup> T. Renner,<sup>(a)</sup>  
 H. Riedesel,<sup>(a)‡</sup> H. G. Ritter,<sup>(b)</sup> A. Warwick,<sup>(b)§</sup> and H. Wieman<sup>(b)</sup>

<sup>(a)</sup>*Nuclear Science Division, Lawrence Berkeley Laboratory, University of California, Berkeley, California 94720*

<sup>(b)</sup>*Gesellschaft für Schwerionenforschung, D-6100 Darmstadt, Federal Republic of Germany*

(Received 1 February 1985)

The particle production (p,d,t,<sup>3</sup>He,<sup>4</sup>He) was studied for 400 and 650 MeV/nucleon Nb + Nb and 400 and 1050 MeV/nucleon Ca + Ca. The chemical freeze-out density of the participants and the entropy produced were deduced for each system. The chemical freeze-out densities are close to normal nuclear density. The entropy production extrapolated for infinite nuclear matter is independent of target-projectile combination at 400 MeV/nucleon and changes little with increasing bombarding energy, but the absolute values are strongly model dependent. The low entropy, when compared to fireball calculations, indicates that compression is present in the collisions. Therefore entropy values in principle can help in the determination of the equation of state for nuclear matter.

### I. INTRODUCTION

One of the ultimate goals in relativistic nuclear physics is to study the behavior of nuclear matter at densities different from the ground state density. It has been suggested that composite particle production<sup>1-4</sup> as well as two-particle correlations<sup>1,5</sup> are relevant observables to determine the size of the participant volume at freeze out. However, the two particle correlation method determines the thermal freeze-out density, the density at which collisions between fragments cease, while the composite particle production method determines the chemical freeze-out density, the density at which composite particles cease to form and break up. Furthermore, there are calculations<sup>6-8</sup> showing that the observed ratio of deuterons to protons can be related to the produced entropy in the system. If the entropy stays constant during the expansion phase,<sup>9,10</sup> the composite particles contain information not only about the freeze out but also about the initial stage of the collision, where the nuclear matter is compressed and hot.

The importance of contributions from heavier fragments ( $A > 4$ ) for the entropy production has been discussed.<sup>7,8</sup> Since the cross section for producing heavy fragments decreases with increasing bombarding energy,<sup>8</sup> this effect is most important at low bombarding energies, while at higher energies the contribution is thought to be negligible. In addition, there are also different suggestions<sup>7,9</sup> as to how the production of composite particles other than deuterons should be counted. Our results are, of course, dependent on the counting scheme used. Up to now all information about composite particle production, except for Ref. 4, has been based on single particle inclusive data which averages over all impact parameters. Most of the models, however, are for infinite nuclear matter which means that it is of great importance to know how the observables vary with the size of the reaction zone to make a reasonable extrapolation for comparison with calculated quantities. In Ref. 4 the deuteron to

proton ratio was reported for the first time to depend strongly on charged particle multiplicity, i.e., on the size of the participant volume. In the present paper we expand upon these results, deduce freeze-out densities and entropies, and compare to model predictions.

### II. EXPERIMENT

The experiments, studying 400 and 1050 MeV/nucleon Ca + Ca and 400 and 650 MeV/nucleon Nb + Nb, were carried out at the Berkeley Bevalac. The data were taken with the Plastic Ball/Wall spectrometer<sup>11</sup> which consists of 815 *DE-E* telescopes each capable of identifying hydrogen and helium isotopes as well as positive pions. The Plastic Ball covers an angular range of 9–160 deg in the laboratory system. The *DE* information is obtained from a 4 mm thick CaF<sub>2</sub> crystal, while the *E* information comes from a 36 cm thick plastic scintillator. Both the *DE* and *E* signals are read out by a common photomultiplier and separated electronically by applying different gates to two analog-to-digital converters (ADC's). Positive pions are detected by recording the positrons coming from the  $\pi^+ \rightarrow \mu^+ \nu$  decay. The forward angular range from 0–9 deg is covered by the Plastic Wall which measures time of flight, *DE*, and the angles of the particles. This part of the detector system only identifies the nuclear charge of the particles and does not identify the different isotopes. The Wall is in part also used to define the event trigger. The data presented here were taken using both a minimum bias trigger and a central collision trigger. The minimum bias trigger means that events in which an intact beam particle appears at 0 deg are rejected, while the central trigger means that events in which any particle with beam velocity appearing within  $\pm 2$  deg in the forward cone are rejected. For all measurements we were using targets with thicknesses between 150 and 200 mg/cm<sup>2</sup>.

### III. COMPOSITE PARTICLE PRODUCTION

#### A. Method

To extract information about the size and density of the participant volume, it is of great importance to exclude the target and projectile spectators in the analysis. It is equally important to cover approximately the same area in phase space when comparing the production rates for different species. The  $d/p$  ratio determines the volume of the system at freeze out, and to determine the density one needs to know the number of baryons in this volume. We define  $N_p$  as the participant baryon charge multiplicity. It also takes into account the participant protons bound in clusters ( $d, t, {}^3\text{He}, {}^4\text{He}$ ). That can easily contribute up to about 40% to  $N_p$ . To determine the participant multiplicity the spectator particles were removed by introducing software cuts in the analysis. In the target region a cut corresponding to 12 MeV/nucleon in the laboratory frame was introduced. This threshold corresponds roughly to the experimental cutoff due to absorption in the target and in the walls of the scattering chamber. In the projectile region the spectator particles were eliminated by applying a cut in the  $p_{\perp}$ -rapidity plane so that all particles with  $p_{\perp}$  less than 150 MeV/c/nucleon in a window around the beam rapidity ( $y_B$ ) were rejected. The window was determined at each energy by using events coming from peripheral collisions and for the four cases studied here it was taken to be  $\pm 0.16$  at  $0.95y_B$ . The factor 0.95 comes from the slowing down of the projectile. In the following the participant baryon charge multiplicity,  $N_p$ , will be abbreviated to proton multiplicity.

The Plastic Ball has full particle identification only in a limited part of the full phase space. Therefore a model is needed to extrapolate from differentially measured to total integrated yields. In this paper the coalescence formalism from Ref. 3 will be used to fit the deuteron to proton ratios and to illustrate how the overlap area in phase space for the different species is determined. By assuming a Boltzmann distribution in momentum space with a parameter  $T$ , one can write the number of deuterons as

$$D = CN^2(2m_N T\pi)^{-3/2} \int 2^{-3/2} \exp(-p_d^2/2m_d T) d^3p \quad (1)$$

and the number of nucleons as

$$N = N(2m_N T\pi)^{-3/2} \int \exp(-p_N^2/2m_N T) d^3p, \quad (2)$$

where  $p_d$ ,  $p_N$ ,  $m_d$ ,  $m_N$  are the momenta and masses of the nucleon and deuteron, respectively,  $T$  is the apparent temperature, and  $C$  is a normalization constant. The same arguments hold for the more general formalism used in Ref. 3. If these two expressions are integrated to infinity one gets

$$D/N = CN \quad (3)$$

which is the basic idea behind the coalescence model. Since the detector system only detects particles in a limited part of phase space, one has to find a region where Eq. (3) is fulfilled. This can be done by choosing an overlap area in the space where the particle momenta have been scaled by  $(1/m)^{1/2}$ , where  $m$  is the mass of the different species ( $p, d, t, {}^3\text{He}, {}^4\text{He}$ ). This follows directly from Eqs. (1) and (2). It can also be thought of as making the com-

parison in the space of (kinetic energy) $^{1/2}$  and angle, which is appropriate because in the thermal model the only relevant parameter is the kinetic energy. However, it can be shown<sup>3</sup> that this scaling is more general. The overlap region was determined for each energy and system by using only the well-identified particles, which means that all particles detected in the Wall as well as those punching through the Ball detectors were rejected.

#### B. Results

The data in Figs. 1 and 2 are presented as ratios, determined in the overlap region, of the produced composite particles ( $d, t, {}^3\text{He}, {}^4\text{He}$ ) to protons as a function of  $N_p$  for the two systems  $\text{Ca} + \text{Ca}$  and  $\text{Nb} + \text{Nb}$  at different bombarding energies. Also shown are the  $N_p/p$  ratios which give the relation between the baryon charge multiplicity and the observed protons. The shown ratios are about 10/1 and the reason for this is that  $N_p$  is determined using all particles, while  $p$  is determined using only those in the overlap region discussed above. From the figures it is seen that all curves show approximately the same

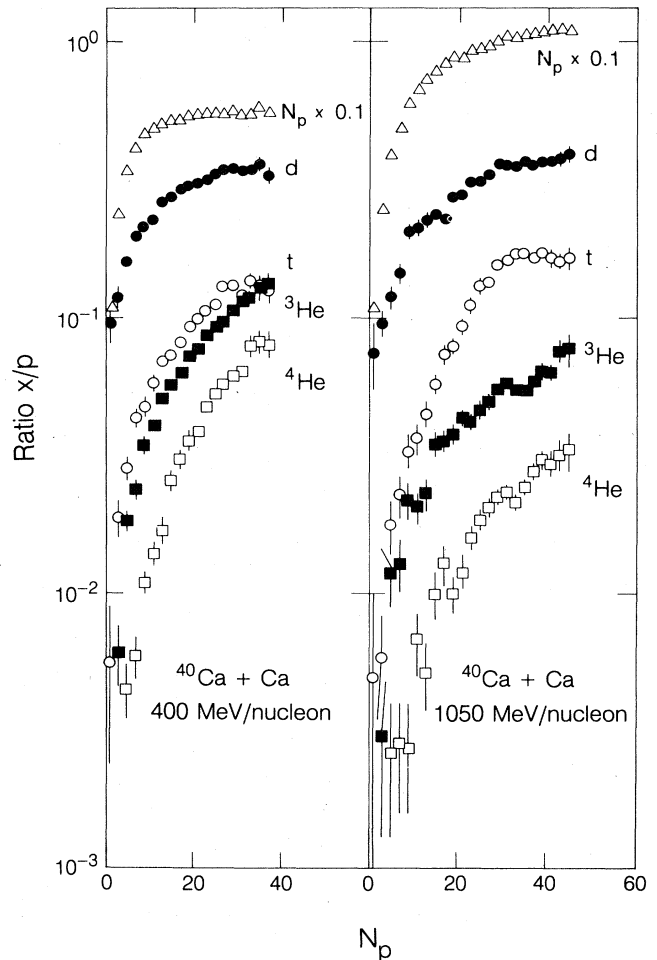


FIG. 1. Ratios of the produced composite particles  $x$  ( $x = d, t, {}^3\text{He}, {}^4\text{He}$ ) to protons as a function of the proton multiplicity ( $N_p$ ) for the system  $\text{Ca} + \text{Ca}$  at 400 and 1050 MeV/nucleon.  $N_p/p$  ratios are also shown.

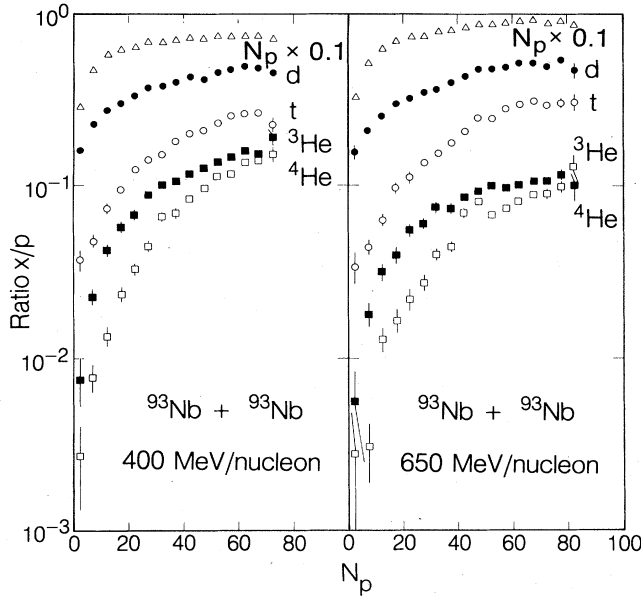


FIG. 2. Ratios of the produced composite particles  $x$  ( $x=d, t, {}^3\text{He}, {}^4\text{He}$ ) to protons as a function of the proton multiplicity ( $N_p$ ) for the system Nb + Nb at 400 and 650 MeV/nucleon.  $N_p$  to  $p$  ratios are also shown.

behavior of increasing cluster production with increasing proton multiplicity and that the curves are leveling off at high  $N_p$  faster for the higher bombarding energies. One can also observe that the ratio  $t/{}^3\text{He}$  is about one for 400 MeV/nucleon Ca (the 1050 MeV/nucleon data are less reliable), but increases when going from Ca to Nb, thus reflecting the neutron excess in the Nb nucleus.

Figure 3 shows the yield of the  $d_{\text{like}}/p_{\text{like}}$  ratio in the overlap region as a function of  $N_p$  for Ca + Ca and Nb + Nb at different bombarding energies. The definition of  $d_{\text{like}}$  was taken from Ref. 9 and is given by

$$d_{\text{like}} = d + \frac{3}{2}(t + {}^3\text{He}) + 3{}^4\text{He}, \quad (4)$$

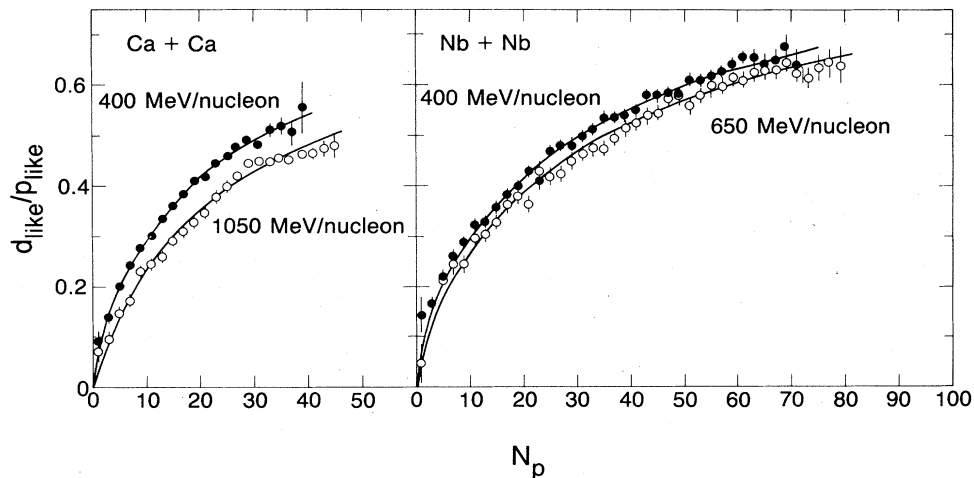


FIG. 3.  $d_{\text{like}}/p_{\text{like}}$  as a function of proton multiplicity ( $N_p$ ) for the two systems Ca + Ca at 400 and 1050 MeV/nucleon and Nb + Nb at 400 and 650 MeV/nucleon. The curves shown are from fits to Eq. (6).

and the quantity  $p_{\text{like}}$  is defined as

$$p_{\text{like}} = p + d + t + 2({}^3\text{He} + {}^4\text{He}). \quad (5)$$

### C. Freeze out

The functional form of the observed  $d_{\text{like}}/p_{\text{like}}$  ratios can be understood in terms of the coalescence model.<sup>1,4,12</sup> In this paper we have used an improved version of the model<sup>1</sup> which is a complete six-dimensional phase space calculation<sup>3</sup> relating the radii of the deuteron and the participant zone to the coordinate space, and relating the temperature of the interacting region to the momentum space. In this model the radius,  $r_p$ , and the temperature,  $T$ , of the interacting region as well as the deuteron radius,  $r_d$ , are related to  $d_{\text{like}}$  and  $p_{\text{like}}$  through

$$d_{\text{like}}/p_{\text{like}} = 6[(A-Z)/Z][1 + 2(r_p/r_d)^2]^{-3/2} \times N_p(1 + \frac{2}{3}m \text{Tr}_d^2)^{-3/2}, \quad (6)$$

where the factor  $(A-Z)/Z$  makes up for the difference between neutron and proton number and  $m$  is the nucleon mass. The radius  $r_p$ , assuming a spherical source, is parametrized as

$$r_p = r_0 \left( \frac{A}{Z} N_p \right)^{1/3},$$

where  $A/Z$  is the factor converting the participant baryon charge multiplicity to participant baryon multiplicity. The reduced radius,  $r_0$ , is then related to the density by  $\rho = 1/(\frac{4}{3}\pi r_0^3)$ . The formula for  $r_p$  differs from the one used in Ref. 4, where  $r_p$  was related to  $\tilde{p}_{\text{like}}$  which was twice the yield of protonlike particles determined in the backward hemisphere of the center of mass system. In this paper  $r_p$  is related to  $N_p$ , which is a more accurate measure of the participant nucleons. The temperature entering Eq. (6) is the apparent temperature obtained from particle spectra (one does not need to have a thermalized system or to know the true temperature, which might be lower than the apparent one due to radial flow<sup>13</sup>). This is

TABLE I. Temperatures used in the fits and the rms radii extracted using Eq. (6).

System	Energy (MeV/nucleon)	$T$ (MeV)	$r_0$ (fm)	$r_d$ (fm)
Ca + Ca	400	50	$1.13 \pm 0.05$	$4.5 \pm 0.4$
Ca + Ca	1050	85	$0.87 \pm 0.06$	$4.1 \pm 0.4$
Nb + Nb	400	50	$1.15 \pm 0.05$	$5.1 \pm 0.5$
Nb + Nb	650	70	$0.97 \pm 0.06$	$4.6 \pm 0.5$

a first order approximation to the original full six-dimensional phase space calculation<sup>3</sup> where both the parallel and longitudinal temperatures enter. In the fits to the observed ratios,  $r_0$  and  $r_d$  were free parameters. The temperature  $T$  was taken to be the mean temperature obtained from Boltzmann fits<sup>13</sup> to the proton spectra at 90 deg in the center of mass systems. The fits to the experimental ratios were done for  $N_p > 5$  and the results are presented as solid curves in Fig. 3. The temperatures used as well as the extracted parameters are given in Table I. For the  $r_d$  parameter (Table I) a trend to smaller values with increasing temperature (i.e., increasing bombarding energy) is not really seen as was predicted in Ref. 14. The  $r_0$  values in the table are the rms values for a Gaussian

density distribution. To convert these values to equivalent sharp sphere radii the listed values have to be multiplied by  $(5/3)^{1/2}$ . The  $r_0^{\text{ssp}}$  values obtained for the four cases studied vary between 1.12 and 1.48 fm. The corresponding freeze-out densities are shown in Fig. 4(a).

The sources of systematic error included are the following:

(i) The temperature turns out not to be a very sensitive parameter, but a decrease in the temperature by 10 MeV from the mean value increases the extracted  $r_0$  and  $r_d$  values by about 8%. This change in  $r_0$  gives rise to a decrease in the determined freeze-out densities by about 20%.

(ii) If the width of the rapidity limits for the cuts in the  $p_{\perp}$ -rapidity plane, determining the  $N_p$  values, are changed by  $\pm 50\%$ , then the shape of the curves in Fig. 3 are only slightly affected. This change gives rise to a change in the extracted  $r_0$  values of about 1% and up to about 8% in the extracted  $r_d$  values. The change in the  $r_0$  values changes the determined freeze-out density by about 3%.

(iii) If the boundaries of the overlap region are changed so that up to 50% more of the particles are thrown away, this affects the extracted  $r_0$  values by about 7% (up to about 10% in the  $r_d$  values). The change in the  $r_0$  values changes the extracted freeze-out densities by about 20%.

The contributions to the errors in the extracted quantities coming from these different sources are summarized in Table III.

#### D. Discussion

The extracted chemical freeze-out densities between 0.5 and 1.0 times normal nuclear matter density deviate from the results obtained from two-particle correlations<sup>15</sup> which give a thermal freeze-out density of about 0.25 times normal nuclear matter density. Some possible explanations for this observed difference might be the following:

(a) In the case of composite particle production which involves bound resonances, a third particle has to be present to conserve momentum and energy, while in the p-p correlation case involving unbound resonances a third particle is not necessary. Because of the necessary presence of the third particle, the chemical freeze-out density determined from the d/p ratios ought to be higher than the thermal freeze-out density extracted from the two-particle correlation analysis.

(b) After the creation of the hot interaction zone it cools and expands. During this stage there are still interactions going on between the particles. The p-p correlations are easily disturbed by small interactions while the bound composite particles are much more immune, thus

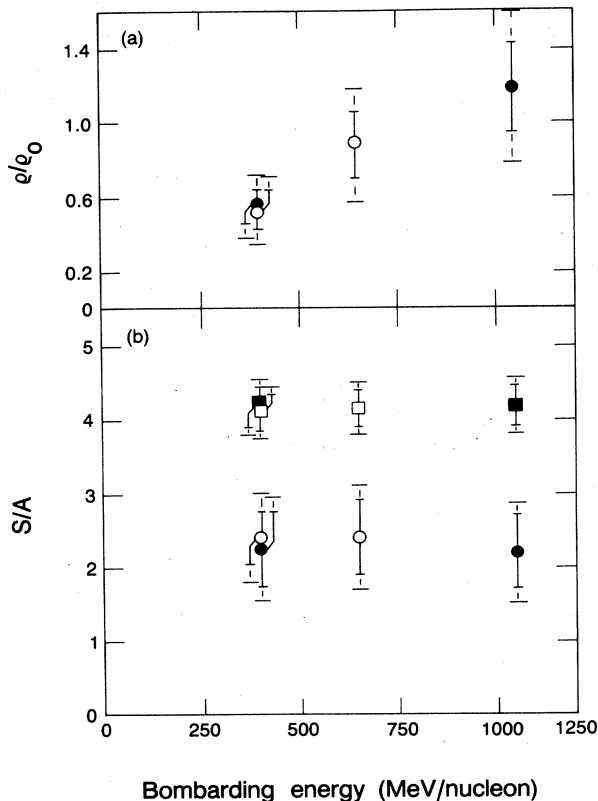


FIG. 4. (a) Chemical freeze-out densities and (b) entropy per nucleon ( $S/A$ ) as a function of bombarding energy for the two systems Ca + Ca at 400 and 1050 MeV/nucleon (filled points) and Nb + Nb at 400 and 650 MeV/nucleon (open points). The smaller error bars are from statistics only, while the bigger ones also include the contributions from systematic errors (see the text for details).

giving a higher chemical freeze-out density than thermal freeze-out density.

From Fig. 3 it is seen that, when comparing the two systems at the same energy and number of participants, the production of composite particles is approximately the same. On the other hand, when comparing the low energy data with the data at the higher energies it is seen that the production of heavier particles decreases with increasing bombarding energy. This is thought to be due to higher temperatures suppressing the production of composite particles.

Figure 3 also shows that the  $d_{\text{like}}/p_{\text{like}}$  ratios increase with increasing proton multiplicity. One might interpret this as being an effect of finite particle number limiting the formation of composites at low multiplicity. However, we did a calculation using a statistical model<sup>16</sup> modified to give a constant temperature as a function of impact parameter. It shows that the finite particle number effect vanishes already at multiplicities around  $N_p = 5$ , while the curves in Fig. 3 continue to rise at much higher proton multiplicities before leveling off. This behavior can instead be interpreted as an effect of the finite size of the deuteron which, at low  $N_p$ , has less overlap with the small participant volume.<sup>4</sup>

#### IV. ENTROPY PRODUCTION FOR INFINITE NUCLEAR MATTER

##### A. Method

There are different models relating the production of composite particles to the produced entropy in the system. We will present here the results extracted from our measured  $d_{\text{like}}/p_{\text{like}}$  ratios using the models of Kapusta<sup>7</sup> and Stöcker<sup>8</sup> and will also briefly discuss the differences between these two methods. In our analysis the number of  $d_{\text{like}}$  and  $p_{\text{like}}$  particles are counted as in the definitions given in Eqs. (4) and (5).

Both models discussed here are calculations for infinite nuclear matter and use the asymptotic values for large  $N_p$  of the ratio  $(d_{\text{like}}/p_{\text{like}})_{\text{asympt}}$  to determine the produced entropy. The asymptotic values of the ratios were determined by using Eq. (6) for infinite proton multiplicity, which then gives

$$(d_{\text{like}}/p_{\text{like}})_{\text{asympt}} = 2.121NA^{-1}R^{-3}(1 + \frac{2}{3}m \text{Tr}_d^2)^{-3/2}, \quad (7)$$

where  $N$  is the number of neutrons,  $A$  is the mass number, and  $R = r_0/r_d$ . With the parameters extracted from the fits shown in Fig. 3 and given in Table I, the asymptotic values were determined for all systems. These values were then used to extract the entropy per nucleon ( $S/A$ ) in accordance with the two models. Following the ideas of Kapusta,<sup>7</sup>  $S/A$  is given by

$$\begin{aligned} S/A = & 0.5213 + 1.5 \ln(9.8X^{-2/3} + 0.7064) \\ & + 5.663X^{-1/3}(1 + 3.566X^{-1/3} + 13.887X^{-2/3} \\ & + 31.108X^{-1})^{-1}, \quad (8) \end{aligned}$$

where  $X$  is related to the average density of nucleons in the six-dimensional phase space. In the Maxwell-Boltzmann limit Eq. (8) reduces to  $S/A = 3.945 - \ln(X)$ . Although this simple equation results in entropy values only 0.1 units smaller than those of Eq. (8), the exact equation was used here. The  $X$  parameter was determined by using the three pieces of information  $d/p$  (defined in Ref. 7),  $d_{\text{tot}}/p$  (defined in Ref. 7), and  $d_{\text{like}}/p_{\text{like}}$  (defined above) and the same fit procedure used and described in Ref. 7. From the calculations of Stöcker,<sup>8</sup>  $S/A$  is given graphically as a function of the asymptotic values of the  $d_{\text{like}}/p_{\text{like}}$  ratios.

##### B. Results

The asymptotic values and the corresponding entropy values  $S/A$  obtained from the two models are given in Table II. The errors given are based on the errors in the fit parameters due to statistics. Also shown are the  $d_{\text{like}}/p_{\text{like}}$  ratios at maximum charge baryon number ( $Z$  of the projectile plus the  $Z$  of the target). These values could be used to extract entropy for comparison with calcula-

TABLE II. The asymptotic  $(d_{\text{like}}/p_{\text{like}})_{\text{asympt}}$  values and the entropy per nucleon ( $S/A$ ) for the different systems extracted by using the two models described in the text. The values are determined using the fit parameters from Table I. Given are also the ratios at maximum charge baryon number  $(d_{\text{like}}/p_{\text{like}})_{\text{max}}$ .

System	Energy (MeV/nucleon)	$(d_{\text{like}}/p_{\text{like}})_{\text{asympt}}$	$(d_{\text{like}}/p_{\text{like}})_{\text{max}}$	$S/A$ (Kapusta)	$S/A$ (Stöcker)
Ca + Ca	400	0.94±0.12	0.53±0.04	4.20±0.25	2.25±0.50
Ca + Ca	1050	0.95±0.19	0.48±0.03	4.20±0.25	2.20±0.50
Nb + Nb	400	1.00±0.13	0.68±0.05	4.15±0.20	2.40±0.35
Nb + Nb	650	1.01±0.15	0.66±0.05	4.15±0.25	2.40±0.50

tions for a finite nuclear system at zero impact parameter. Before the big systematic difference in the extracted entropy values is discussed, the contribution to the errors due to systematics is presented in the following:

(i) As mentioned above, the uncertainty in the cuts determining the  $N_p$  values changes the extracted  $r_0$  and  $r_d$  values. Due to this effect the determined asymptotic values change by about 2%. This gives rise to a change in the determined entropy values of up to 4% for the model of Stöcker.<sup>8</sup>

(ii) The change in the extracted  $r_0$  due to changes in the used temperature parameter does not contribute to the error in the asymptotic values, because the change in temperature also changes the extracted  $r_d$  values in the same direction as  $r_0$ , giving no net change in the calculated asymptotic values or in the determined entropy values.

(iii) If the boundaries of the overlap region for the different species are changed in the same way as was described above, the asymptotic values of the deuteron to proton ratios change by about 20%. This change gives rise to a change in the extracted entropy values due to the model of Stöcker<sup>8</sup> by about 20% and by about 4% due to the model of Kapusta.<sup>7</sup> The contributions to the errors in the extracted quantities coming from the different sources mentioned above are given in Table III.

Figure 4(b) shows the entropy per nucleon extracted from the different models as a function of bombarding energy. The lower points are from the model by Stöcker<sup>8</sup> and the upper ones are from the model by Kapusta.<sup>7</sup> Because we have extrapolated the ratios to infinite multiplicity before calculating the entropies both models say that at the same energy/nucleon the produced entropy is independent of target projectile combination, as one would expect. The most striking feature of Fig. 4(b) is the big difference in entropy obtained from the two models, even though the basic physics going into the two models is essentially the same.

### C. Discussion

Both models are quantum-statistical calculations including the effect of the finite volume of the particles. The model of Kapusta<sup>7</sup> predicts the number of real deuterons and deuteron pairings contained in heavier clusters but it does not say what these clusters are. The model of Stöcker<sup>8</sup> (see also Fig. 6 in Ref. 17) includes the production of heavy clusters up to  $A=20$  as well as the decay of all unbound resonances for these species. This model also

includes the contribution to the entropy from the production of pions and deltas, while in the model of Kapusta<sup>7</sup> these are not taken into account. The contribution from pions and deltas is of course most important at the highest bombarding energies.

If the unbound clusters are responsible for the difference in the extracted entropy at the lower bombarding energies then the disagreement should decrease with increasing bombarding energy, but this behavior is not seen in Fig. 4(b). The difference seen at the highest bombarding energy is probably too large to be explained by the production of pions and deltas which is not included in the model of Kapusta.<sup>7</sup>

If the contributions from quantum statistics, unbound resonances, heavy fragments, pions, and deltas are turned off in the calculations by Stöcker,<sup>8</sup> then the resultant entropy values agree very well with the ones obtained from the model by Kapusta.<sup>7</sup> It is, however, not clear which of the above-mentioned effects contribute most to the difference in the extracted entropy values.

It is also known that at the highest proton multiplicity the experimental data<sup>18</sup> account for most of the charges in the system not allowing much room for heavy clusters. This is in agreement with the calculation of Stöcker<sup>8</sup> which gives about 3% of all charges in clusters heavier than alphas. For infinite nuclear matter the same calculation gives about 15% of all charges in fragments heavier than alphas, indicating that the production of heavy fragments cannot alone be responsible for the observed difference in the extracted entropies.

## V. EQUATION OF STATE

If the produced entropy stays constant during the expansion, then it contains information on the equation of state which controlled the reaction. Without an observable for the density reached in the reaction, one is forced to rely on models relating the bombarding energy to the density. In the nuclear fireball model<sup>12</sup> all available kinetic energy goes into thermalization and thus no compression or density increase is implied. This results, for a cluster freeze-out density of  $\rho/\rho_0=1$ , in the entropy and temperature values shown in Figs. 5(a) and (b) as the dashed curves (the choice of a lower freeze-out density would result in even larger entropy values). The fireball calculations were done following the model of Ref. 8. As

TABLE III. The contributions to the errors in the extracted quantities coming from different sources. The values given are upper limits. For details see the error discussions in the text.

Quantity	Statistics	$N_p$ changes	Temperature changes	Boundary changes
$r_0$	$\pm 7\%$	$\pm 1\%$	$\pm 8\%$	$\pm 6\%$
$r_d$	$\pm 15\%$	$\pm 8\%$	$\pm 9\%$	$\pm 10\%$
Asymptotic	$\pm 20\%$	$\pm 2\%$	small	$\pm 20\%$
$d_{\text{like}}/p_{\text{like}}$				
Density	$\pm 20\%$	$\pm 3\%$	$\pm 20\%$	$\pm 20\%$
Entropy (Stöcker)	$\pm 20\%$	$\pm 4\%$	small	$\pm 20\%$
Entropy (Kapusta)	$\pm 4\%$	small	small	$\pm 4\%$

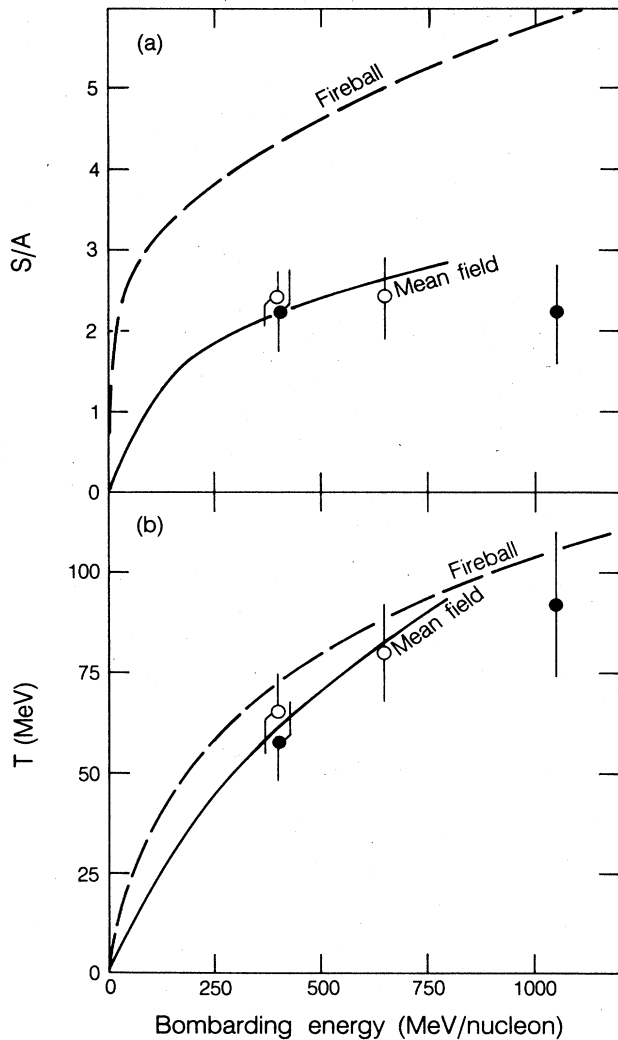


FIG. 5. (a) Entropy per nucleon ( $S/A$ ), extracted using the model of Stöcker (Ref. 8) and (b) the experimentally determined apparent temperatures at maximum proton multiplicity as a function of bombarding energy (the symbols have the same meaning as in Fig. 4). The curves labeled Fireball and Mean are results of calculations described in the text.

can be seen from the comparison with the entropy values extracted from the data by the Stöcker method,<sup>8</sup> this fireball prediction without compression is much too large.

In the hydrodynamical model some of the available kinetic energy naturally goes into compressional energy. Hydrodynamical calculations using an equation of state based on the relativistic mean field theory of Ref. 19 show very good agreement with the experimentally extracted entropy values using the method of Ref. 8. The choice of the equation of state does not change the entropy production significantly as was pointed out by Stöcker *et al.*<sup>20</sup> (An assumption of a softer equation of state results in slightly larger entropy values.) To differentiate and determine more precisely the proper equation of state is not

possible partly due to the systematic errors in the method of extrapolation to infinite matter. We emphasize the need for methods and models describing the finite size of nuclear systems, where our data are of higher precision. However, from Fig. 5(a) it is clearly seen that compression has to be present to explain the produced entropy in the collision.

In addition to the extracted entropy, apparent temperatures have been determined from the proton spectra at 90 deg in the center of mass system.<sup>13</sup> This introduces a further specification of the thermodynamical properties of the reaction zone, however, unfortunately without an improvement in the knowledge of the density reached in the collision. The comparison between the temperatures from the calculations described above and the experimentally determined apparent ones is shown in Fig. 5(b). The latter ones are the values extracted at maximum charged baryon multiplicity. The dashed curve is the result of the fireball calculation without compression and is close to the observed maximum apparent temperatures. The solid curve represents the temperature predicted from the hydrodynamical calculation using an equation of state based on the relativistic mean field theory of Ref. 19, but without pions included.

## VI. CONCLUSIONS

We have presented data on composite particle production as a function of multiplicity for different colliding systems and energies. These data can be understood by the improved coalescence model taking the radius and temperature of the participant region, as well as the radius of the deuteron, into account. The obtained radii for the interacting volume give chemical freeze-out densities close to normal nuclear density. We have also presented results on entropy production in the systems studied by considering two different models for the determination of the entropy. The results show large differences which clearly show that the determination of entropy produced in nuclear collisions is strongly model dependent. Favoring the model by Stöcker,<sup>8</sup> we conclude that compression is achieved in the collision and that the no-compression fireball model produces too much entropy. It is, however, not possible to make a further distinction between compressional potential and compressional kinetic energy since these two quantities are not independent of each other. The globally measured  $d/p$  ratios, together with a proper method for the entropy determination, allows one, in principle, to distinguish between different equations of state. A determination of the proper equation of state from data, however, would be improved by a model which does not need to extrapolate from the finite size volumes in nuclear collisions to that of infinite matter, but rather uses the higher accuracy of the experimental data themselves. The findings that compression is needed to explain the entropy values can be related to the pressure effect observed in form of collective flow (side splash).<sup>21</sup> The flow phenomenon can now be connected with nuclear compression and not thermal pressure alone.

## ACKNOWLEDGMENTS

We are grateful for the continuous support of Professor R. Bock. H. Stöcker is acknowledged for performing the calculations referred to in this paper and for many valu-

able and stimulating discussions. We also thank J. Boguta, M. Gyulassy, and J. Kapusta for many helpful suggestions. This work was supported in part by the U.S. Department of Energy under Contract DE-AC03-76SF00098.

\*Present address: Institut für Kernphysik, Universität Münster, D-4400 Münster, Federal Republic of Germany.

†Also at Fachbereich Physik, Philipps Universität Marburg, D-3550 Marburg 1, Federal Republic of Germany.

‡Present address: Springer Verlag, Berlin, Federal Republic of Germany.

§Present address: Lawrence Berkeley Laboratory, University of California, Berkeley, CA 94720.

<sup>1</sup>H. Sato and K. Yazaki, Phys. Lett. **98B**, 153 (1981).

<sup>2</sup>A. Z. Mekjian, Phys. Rev. C **17**, 1051 (1978).

<sup>3</sup>M. Gyulassy and E. Remler (unpublished).

<sup>4</sup>H. H. Gutbrod, H. Löhner, A. M. Poskanzer, T. Renner, H. Reidesel, H. G. Ritter, A. Warwick, F. Weik, and H. Wieman, Phys. Lett. **127B**, 317 (1983).

<sup>5</sup>S. E. Koonin, Phys. Lett. **70B**, 43 (1977).

<sup>6</sup>P. J. Siemens and J. I. Kapusta, Phys. Rev. Lett. **43**, 1468 (1979).

<sup>7</sup>S. Das Gupta, B. K. Jennings, and J. I. Kapusta, Phys. Rev. C **26**, 274 (1982); J. I. Kapusta, *ibid.* **29**, 1735 (1984).

<sup>8</sup>H. Stöcker, G. Buchwald, G. Graebner, P. Subramanian, J. A. Maruhn, W. Greiner, B. V. Jacak, and G. D. Westfall, Nucl. Phys. **A400**, 63c (1983); B. V. Jacak, H. Stöcker, and G. D. Westfall, Phys. Rev. C **29**, 1744 (1984).

<sup>9</sup>G. Bertsch and J. Cugnon, Phys. Rev. C **24**, 2514 (1981).

<sup>10</sup>J. I. Kapusta, Phys. Rev. C **24**, 2545 (1981).

<sup>11</sup>A. Baden, H. H. Gutbrod, H. Löhner, M. R. Maier, A. M. Poskanzer, T. Renner, H. Reidesel, H. G. Ritter, H. Spieler, A. Warwick, F. Weik, and H. Wieman, Nucl. Instrum.

Methods **203**, 189 (1982).

<sup>12</sup>H. H. Gutbrod, A. Sandoval, P. I. Johansen, A. M. Poskanzer, J. Gosset, W. G. Meyer, G. D. Westfall, and R. Stock, Phys. Rev. Lett. **37**, 667 (1976).

<sup>13</sup>H.-Å. Gustafsson, H. H. Gutbrod, B. Kolb, H. Löhner, B. Ludewigt, A. M. Poskanzer, T. Renner, H. Reidesel, H. G. Ritter, A. Warwick, and H. Wieman, Phys. Lett. **142B**, 141 (1984).

<sup>14</sup>H. Schultz, G. Röpke, K. Gudima, and V. D. Toneev, Phys. Lett. **124B**, 458 (1983).

<sup>15</sup>H.-Å. Gustafsson, H. H. Gutbrod, B. Kolb, H. Löhner, B. Ludewigt, A. M. Poskanzer, T. Renner, H. Reidesel, H. G. Ritter, A. Warwick, and H. Wieman, Phys. Rev. Lett. **53**, 544 (1984).

<sup>16</sup>G. Fai and J. Randrup, Nucl. Phys. **A404**, 551 (1983).

<sup>17</sup>H. Stöcker, Nucl. Phys. **A418**, 587c (1984).

<sup>18</sup>H.-Å. Gustafsson, H. H. Gutbrod, B. Kolb, H. Löhner, B. Ludewigt, A. M. Poskanzer, T. Renner, H. Reidesel, H. G. Ritter, A. Warwick, F. Weik, and H. Wieman, Lawrence Berkeley Laboratory Report LBL-16870, 1984, pp. 189 and 190.

<sup>19</sup>J. Boguta and H. Stöcker, Phys. Lett. **102B**, 289 (1983).

<sup>20</sup>H. Stöcker, M. Gyulassy, and J. Boguta, Phys. Lett. **103B**, 269 (1981).

<sup>21</sup>H.-Å. Gustafsson, H. H. Gutbrod, B. Kolb, H. Löhner, B. Ludewigt, A. M. Poskanzer, T. Renner, H. Reidesel, H. G. Ritter, A. Warwick, F. Weik, and H. Wieman, Phys. Rev. Lett. **52**, 1590 (1984).